

# MicroRNA29a Treatment Improves Early Tendon Injury

Ashlee E. Watts,<sup>1,4</sup> Neal L. Millar,<sup>2,4</sup> Josh Platt,<sup>1</sup> Susan M. Kitson,<sup>2</sup> Moeed Akbar,<sup>2</sup> Raquel Rech,<sup>1</sup> Jay Griffin,<sup>1</sup> Roy Pool,<sup>1</sup> Tom Hughes,<sup>3</sup> Iain B. McInnes,<sup>2</sup> and Derek S. Gilchrist<sup>2</sup>

<sup>1</sup>The Comparative Orthopedics and Regenerative Medicine Laboratory, Texas A&M University, College Station, TX 77843, USA; <sup>2</sup>Institute of Infection, Immunity, and Inflammation, College of Medicine, Veterinary, and Life Sciences, University of Glasgow, Glasgow G12 8TA, UK; <sup>3</sup>Liphook Equine Hospital, Forest Mere, Liphook GU30 7JG, UK

**Tendon injuries (tendinopathies) are common in human and equine athletes and characterized by dysregulated collagen matrix, resulting in tendon damage. We have previously demonstrated a functional role for microRNA29a (miR29a) as a post-transcriptional regulator of collagen 3 expression in murine and human tendon injury. Given the translational potential, we designed a randomized, blinded trial to evaluate the potential of a miR29a replacement therapy as a therapeutic option to treat tendinopathy in an equine model that closely mimics human disease. Tendon injury was induced in the superficial digital flexor tendon (SDFT) of 17 horses. Tendon lesions were treated 1 week later with an intralesional injection of miR29a or placebo. miR29a treatment reduced collagen 3 transcript levels at week 2, with no significant changes in collagen 1. The relative lesion cross-sectional area was significantly lower in miR29a tendons compared to control tendons. Histology scores were significantly better for miR29a-treated tendons compared to control tendons. These data support the mechanism of microRNA-mediated modulation of early pathophysiologic events that facilitate tissue remodeling in the tendon after injury and provides a strong proof of principle that a locally delivered miR29a therapy improves early tendon healing.**

## INTRODUCTION

Dysregulated tissue repair and inflammation characterize many musculoskeletal pathologies, including tendon disorders in both human and equine practice.<sup>1–4</sup> Tendon injuries remain a significant problem in equine practice, comprising the most common musculoskeletal injury in racehorses. Injury to the superficial digital flexor tendon (SDFT), most often involving the metacarpal segment of the forelimb tendon, is one of the most frequent causes of lameness of athletic horses internationally, with a reported frequency of 10%–30%.<sup>5,6</sup>

The immune system plays a crucial role in the regulation of tissue remodeling by coordinating complex signaling networks that facilitate transcriptional regulation of extracellular matrix (ECM) components as an adaptive response to environmental cues. Inflammatory mediators are considered crucial to the onset and perpetuation of tendinopathy.<sup>7–9</sup> Expression of various cytokines has been demonstrated in

inflammatory cell lineages and tenocytes, suggesting that both infiltrating and resident populations participate in pathology.<sup>10–12</sup> Additionally, evidence suggests a balance exists between proinflammatory and proresolving mediators that may ultimately define the extent to which equine tendinopathy develops and subsequently repairs.<sup>13,14</sup>

Recent work has identified the importance of tissue microenvironments and the interaction of immune mediators in inflammatory/stromal cell crosstalk.<sup>15</sup> MicroRNAs are small, non-coding RNAs that suppress gene expression at the post-transcriptional level by inhibiting translation and/or inducing mRNA degradation.<sup>16</sup> A single microRNA can regulate the expression of multiple target mRNAs through sequence binding. Emerging studies highlight microRNAs as key epigenetic regulators of integrated mammalian cell functions.<sup>17,18</sup> Specific microRNAs have emerged that particularly regulate cytokine networks while orchestrating proliferation and differentiation of stromal lineages that determine ECM composition.<sup>19</sup> microRNAs have provoked extensive interest as regulators of musculoskeletal diseases, although their precise contributions to complex disease pathways remains uncertain.<sup>20</sup> miR-210 has been reported as a crucial regulator of angiogenesis,<sup>21</sup> a key factor in tendon disease, and it accelerated healing of the tendon in an Achilles tendon rodent injury model<sup>22</sup> while additionally causing upregulation of vascular endothelial factor, fibroblast growth factor, and type I collagen in the same model system. microRNAs designed and engineered according to genetic sequences of transforming growth factor  $\beta$ 1 (TGF- $\beta$ 1) and injected in the chicken tendon injury model achieved downregulation of TGF- $\beta$ 1 expression in vitro and in vivo.<sup>23</sup> Some compounds can regulate endogenous microRNA expression, which may confer therapeutic value. One such study demonstrated that miR29b

Received 18 June 2017; accepted 25 July 2017;  
<http://dx.doi.org/10.1016/j.ymthe.2017.07.015>.

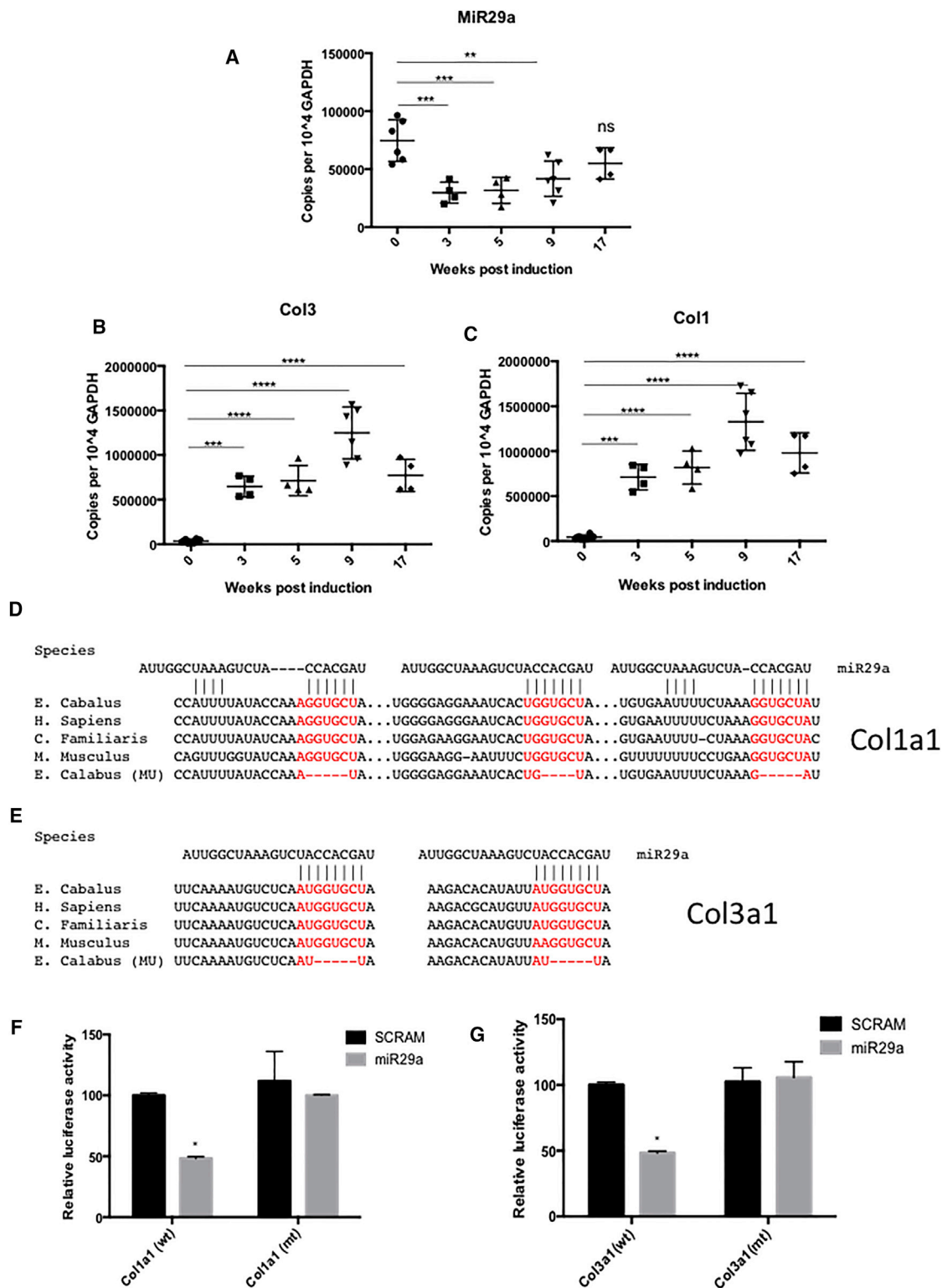
<sup>4</sup>These authors contributed equally to this work.

**Correspondence:** Derek S. Gilchrist, PhD, Institute of Infection, Immunity, and Inflammation, College of Medicine, Veterinary, and Life Sciences, University of Glasgow, 120 University Avenue, Glasgow G12 8TA, UK.

**E-mail:** [derek.gilchrist@glasgow.ac.uk](mailto:derek.gilchrist@glasgow.ac.uk)

**Correspondence:** Neal L. Millar, PhD, FRCSEd(Tr&Ortho), Institute of Infection, Immunity, and Inflammation, College of Medicine, Veterinary, and Life Sciences, University of Glasgow, 120 University Avenue, Glasgow G12 8TA, UK.

**E-mail:** [neal.millar@glasgow.ac.uk](mailto:neal.millar@glasgow.ac.uk)



(legend on next page)

mediated chitosan-induced prevention of tendon adhesion after rodent Achilles tendon injury surgery by regulating the TGF- $\beta$ 1-Smad3 pathway.<sup>24</sup>

We have previously demonstrated a functional role for miR29a as a post-transcriptional regulator of collagen in murine and human tendon injury.<sup>25</sup> Given the translational potential, we designed a randomized blinded trial to evaluate the potential for miR29a replacement therapy as a therapeutic option to treat tendinopathy, utilizing an equine collagenase model considered analogous to human tendon disease.

## RESULTS

### miR29a Expression in Equine Tendinopathy Model

We found that miR29a was significantly ( $p < 0.01$ ) downregulated throughout the time course of the induced tendinopathy model (Figure 1A). Additionally, we noted a significant differential regulation of collagen 1 and 3 transcripts throughout the time course (Figures 1B and 1C). The most notable changes were in the collagen 3 transcript early in the model, which was upregulated 80-fold at week 3 and 25-fold at week 5 post induction, which was maintained >30-fold at weeks 9 and 17. This was in contrast to collagen 1 transcripts, which were upregulated significantly less ( $p < 0.05$ ) at early time points (13-fold at 3 weeks and 9-fold at 5 weeks;  $p < 0.05$  versus collagen 3 transcript), which was reversed at weeks 9 (26-fold) and 17 (24-fold).

### Regulation of Collagen Expression by miR29a Is Conserved in Equine Tenocytes

Sequence analysis revealed that the miR29a-binding sites in collagen 1 and 3 transcripts previously described in humans and mice are conserved in horses (Figures 1D and 1E). To confirm the activities of these predicted miR29a-binding sites, a series of luciferase reporter constructs containing wild-type and mutated miR29a-binding sites were made. Overexpression of miR29a decreased luciferase activity in HEK cells transfected with wild-type but not mutated plasmids, demonstrating that both col1a1 and col3a1 are bona fide miR29a targets (Figures 1F and 1G). To test whether miR29a indeed regulates the levels of candidate target mRNAs in disease-relevant cells, we transfected primary equine tenocytes with a miR29a mimic. miR29a manipulation selectively regulated collagen 3 ( $p < 0.01$ ) but not collagen 1 mRNA (Figures 2A and 2B). This is in keeping with our previous observations in human tenocytes, which showed that miR29a-binding sites are excised from collagen 1 transcripts due to the use of an alternative proximal polyadenylation signal.<sup>25</sup> Comparison of the poly(A) sites in both col1a1 and col3a1 showed that the polyadenylation signals and the sequences that flank them are iden-

tical in other mammalian species, including horses and dogs, suggesting that this alternative polyadenylation is conserved in these species (Figures 2C–2F). To test this, the 3' ends of collagen 1 and 3 transcripts were characterized using 3' rapid amplification of cDNA ends (RACE). Sequence analysis showed that both collagen 1 and 3 utilized the same conserved polyadenylation signals found in the corresponding human transcripts (Figures 2G and 2H). Together, these results support the idea of a common molecular pathogenic process driven by the loss of miR29a in the development of tendinopathy in humans and horses. This finding raises the possibility that re-introduction of miR29a could have significant therapeutic benefit in the healing of tendon lesions.

### miR29a Treatment Improves Early Tendon Healing

The study consisted of two randomly assigned groups, group A (miR29a mimic;  $n = 9$ ; five males, four females; miR29a) and group B (placebo-treated tendons;  $n = 8$ ; five males, three females; control [CONT]), with the study timeline detailed in Figure 3A.

### qPCR

miR29a treatment specifically suppressed collagen 3 at week 2 ( $p = 0.01$ ) and showed a trend toward reduction at week 4 ( $p = 0.06$ ) (Figures 3B and 3C). Importantly, in keeping with our in vitro data, miR29a treatment caused no significant changes in collagen 1 at any time points in this equine model.

### Ultrasound

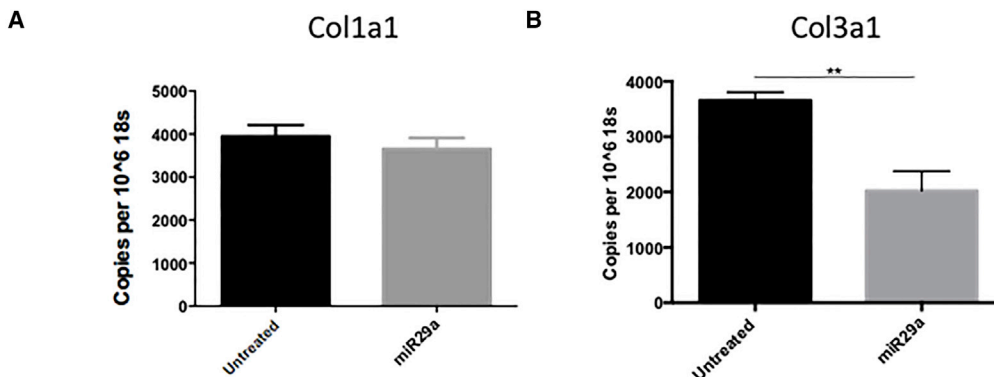
Normalized lesion CSA was significantly lower in miR29a-treated tendons compared to control tendons at  $t = 6, 12,$  and  $16$  weeks ( $p < 0.05$ ) and showed a trend for smaller CSA at  $t = 8$  weeks ( $p = 0.1$ ) (Figure 4A). Normalized relative lesion CSA was significantly lower in miR29a tendons compared to control tendons at  $t = 6, 8, 12,$  and  $16$  weeks ( $p < 0.05$ ) (Figure 4B). Subjective blinded ultrasound (US) scoring showed significant less SC thickening and more normal tissue architecture at weeks 12 and 16 in the miR29a tendons compared to the control tendons (Figure 4C; Table 1).

### MRI

Tendon lesions were identified by increased T2-weighted signal intensity in all tendons (Figures 5A and 5B). Tendon CSA made on magnetic resonance images were not significantly different between groups (Figure 5B). However, there was a trend ( $p = 0.07$ ) of reduced relative CSA and reduced lesion CSA of miR29a-treated tendons compared to those of control tendons at weeks 4, 6, 12, and 16. Additionally, the T<sub>2</sub> relaxation times were significantly ( $p < 0.05$ ) greater in control tendons at 12 weeks (miR29a,  $57.9 \pm 15$ ; control,  $218.9 \pm 74.6$ ) (Figure 5C).

## Figure 1. miR29a Is Dysregulated in Equine Tendinopathy and Targets col1a1 and col3a1 via Conserved Binding Sites

(A–C) miR29a (A), col3a1 (B), and col1a1 (C) expression in an equine tendinopathy model at 3, 5, 9, and 17 weeks post lesion induction. Data for mRNA are total copy number of gene versus GAPDH housekeeping gene in duplicate samples. \* $p < 0.05$  and \*\* $p < 0.01$  versus control (ANOVA). (D and E) Sequence alignments of miR29a with its predicted binding sites in col1a1 (D) and col3a1 (E). Seed regions are shown in red. (F and G) Luciferase activity in HEK293 cells co-transfected with wild-type or mutated col1a1 (F) or col3a1 (G) 3' UTR luciferase reporter and miR29a or scrambled control mimics. Activities were normalized to control and values expressed as % of scrambled controls ( $n = 3$ ). Data analyzed by Mann-Whitney U Test, \* $p < 0.05$  versus scrambled control.

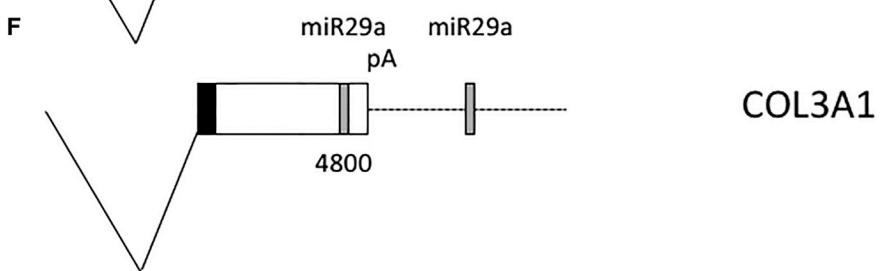
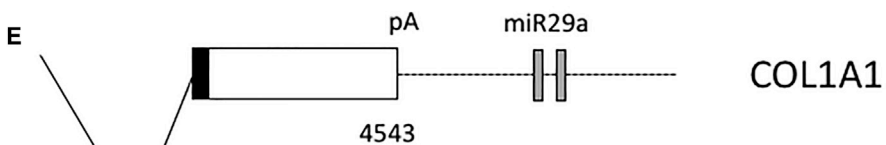


**C** Coll1a1 polyA  
 E. Cabalus AAAAAAGAAUAAUAAAUAACUUUUUUAAAAAGGAAG  
 H. Sapiens AAAAAAGAAUAAUAAAUAACUUUUUUAAAAAGGAAG  
 C. Familiaris AAAAAAGAAUAAUAAAUAACUUUUUUAAAAAGGAAG  
 M. Musculus AAAAAAGAAUAAUAAAUAACUUUUUUAAAAAGGAAG

COL1A1

**D** Col3a1 polyA  
 E. Cabalus UUUCAAAUGUCUCAUUGGUGCUAUAAUAAAUAAAC  
 H. Sapiens UUUCAAAUGUCUCAUUGGUGCUAUAAUAAAUAAAC  
 C. Familiaris UUUCAAAUGUCUCAUUGGUGCUAUAAUAAAUAAAC  
 M. Musculus UUUCAAAUGUCUCAUUGGUGCUAUAAUAAAUAAAC

COL3A1



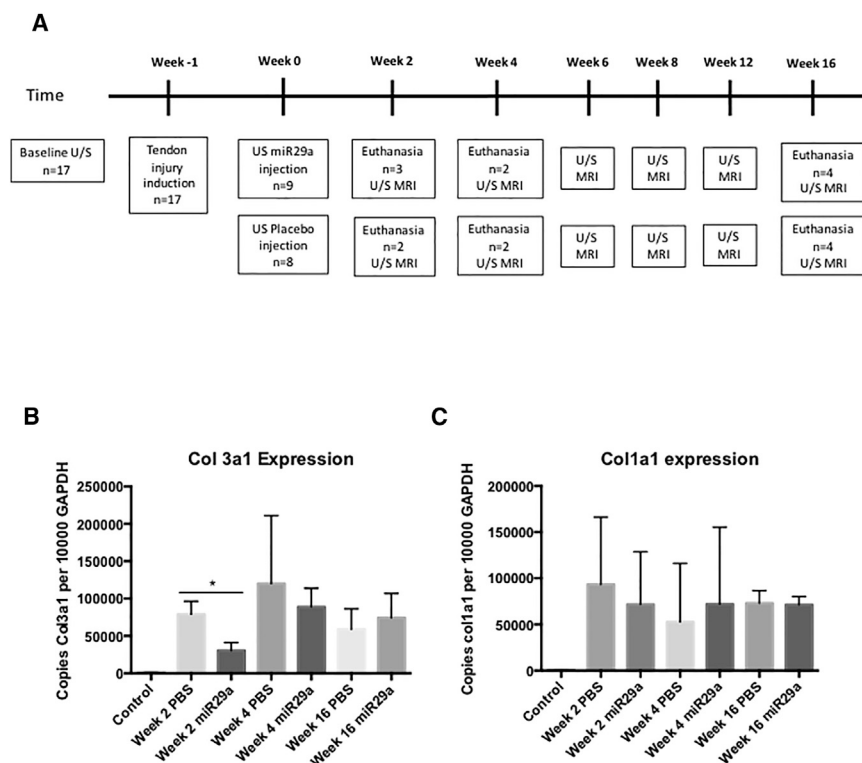
**G** 3'RACE COL1A1  
 GTCGTCTTCTGTAAACTCCCTCCGCCCCAACCTGGCTCCCTCCCACCCAGTCCACTTGCCTCCCTGGAAACAGAC  
 AAACAACCCAACTGAACCCCCAAAAAGCCAAAAAATGGGAGACAATTTCACATGGACTTTGGAAATATTTTTTCCT  
 TTGCATTCATCTCTCAAACCTAGTTTTTATCTTTGACCAACTGACCATGACAAAAACAAAAGTGATCAACCTTACC  
 AAAAAAAAAAAAAAGATAATAATATAACTTTTTAAAAAGGAAGAAAAAAAAAAAAAAAAAAAAAAAAA

**H** 3'RACE COL3A1  
 GCCCTTCTATGATGTTGGTGGTCCATGATCAAGAAATTCGGTGTGGACATGGCCCTGTTTGCTTTTTATAACCAAACCTCT  
 TATCTGAAACCCAGCAAAAAGTTTCACACTCCATATGTGTTCCCTCTGTTTAAATTTTGCAACCAAGTACAAGTGACCA  
 ACTAAATCCAGTATTTATTTCCAAAATTTTTGAAAAAGTATAATTTGACAAAAATGATGCTTTTTTTCCTGTCCCA

miR29a binding site

CCAAATACAGTTCAAATGCTTTTTGTCTATTTTTTACCAATTCCAATTTCAAATGTCTCAATGGTGTATATAAAT  
 AAACCTCAACACTCTTACAAGAAAAAAAAAAAAAAAAAAAAAAAAA

(legend on next page)



### Gross Dissection and Histology

No peritendinous adhesions were noted during dissection in either group. Cumulative histology scores were significantly better for miR29a-treated tendons compared to control tendons (Figures 6A and 6B) at weeks 2 and 16 utilizing the modified Bonar score (cell density, vascularity, linear fiber, and polarized collagen). Tendons from both groups were visibly enlarged, centered at 16 cm distal to the accessory carpal bone (DACB), and had minimal peritendinous reaction. Although no scores were assigned, miR29a-treated tendons appeared smaller at 16 cm DACB and had less peritendinous reaction, and treatment injection sites were less obvious (Figure 6C).

### DISCUSSION

The molecular processes underpinning the development of collagen 3 over-production seen in tendinopathy have been evolutionarily conserved in mammalian species, demonstrating their biological importance. Here, we showed that the injury-induced loss of miR29a from tenocytes previously reported in humans also occurs in collagenase-induced tendinopathy in horses and that this

### Figure 3. miR29a Treatment Targets col3a1 with No Effect on col1a1 in Early Tendon Healing In Vivo

(A) Study timeline. (B and C) qPCR of col3a1 (B) and col1a1 (C) of tendon lesion samples expressed as copies per 10,000 copies of GAPDH. Week 2, n = 3, week 4, n = 2, and week 16, n = 4. \*\*p < 0.01 versus scrambled control (one-way ANOVA).

inversely correlates with collagen 3 expression. We have demonstrated that, as is the case in humans, miR29a has the potential to target both collagen 1 and 3. Despite this, only collagen 3 expression is decreased by the miR29a overexpression in equine tenocytes. A detailed characterization of col1a1 and col3a1 transcripts reveals that col1a1 utilizes an alternative poly(A) signal that truncates its 3' UTR with the loss of all three miR29-binding sites. This means that in equine tenocytes, only collagen 3 is regulated by miR29a, a situation that mirrors that previously described in humans. These findings raised the possibility that re-introduction of miR29a into the tendinopathic environment could reduce collagen 3 production, leading to improved tendon healing.

To test this, we designed a blinded, placebo-controlled, experimental trial of an equine model that revealed clinically relevant improvement in the healing of early tendon injury after intralesional injection of miR29a.

Recent studies highlight microRNAs as key regulators of leukocyte function and differentiation of stromal cells that determine extracellular matrix composition.<sup>20,26,27</sup> Our data demonstrate a functional role for miR29a as a post-transcriptional regulator of collagen in equine tendon injury. Despite its many similarities, the collagenase model of tendon injury does not totally mimic the insidious and degenerate etiopathogenesis of many forms of naturally occurring tendon injury in man. However, the clinical relevance of this model to the final acute disruption after months or years of chronic tendon injury is supported by the evaluation of gross, biochemical, and histopathological changes, clinical signs, mechanical characteristics, and MRI and ultrasonographic findings following the induction of injury.<sup>28,29</sup> Additionally, the collagenase model allows the generation of a homogeneous tendon lesion in a controlled group of animals and, therefore, improved ability to detect differences between the treated

### Figure 2. miR29a Preferentially Targets col3a1 over col1a1 in Equine Tenocytes

(A and B) Copies col1a1 (A) and col3a1 (B) transcripts levels after transfection with miR29a and scrambled (control) mimics normalized to 10<sup>6</sup> copies of 18S. This was repeated in three independent experiments. \*\*p < 0.01 versus scrambled control (Student's t test). (C and D) sequence alignments of predicted col1a1 (C) and col3a1 (D) polyadenylation signals (underlined). (E and F) Diagram of alternative polyadenylated 3' UTRs from col1a1 (E) and col3a1 (F), showing the positions of miR29a-binding sites and predicted polyadenylation signals (pA). (G and H) 3' RACE sequences of col1a1 (G) and col3a1 (H) transcripts cloned from equine tenocytes. Stop codon is shown in red, poly(A) signals are underlined, the poly(A) tail is shown in bold, and the miR29a-binding site is shown in blue.

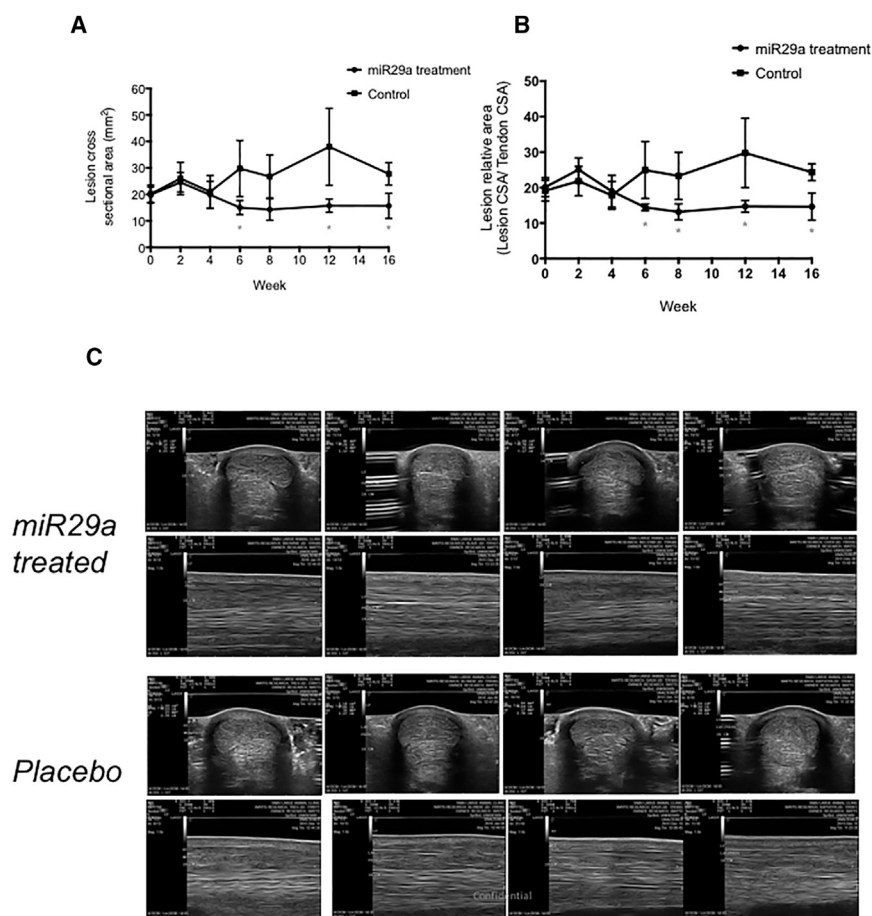


**Figure 4. Ultrasound Tendon Healing Post miR29a Treatment**

(A and B) Normalized lesion (A) and lesion relative to tendon cross-sectional area (CSA) (B) for miR29a and placebo-treated tendons (control) at time points post treatment injection in weeks. \* $p < 0.05$  versus control (one-tailed Student's *t* test). (C) Transverse and longitudinal ultrasound images 16 cm DACB, 16 weeks post treatment with miR29a- or placebo-treated tendons.

tissue quality, collagen content, and collagen orientation due to miR-29a replacement.

The standard of care for tendon and ligament injury in equine clinical medicine is conservative therapy, based on minimizing exercise and anti-inflammatory medication. Novel methods have focused on regenerative medicine approaches with either platelet rich plasma (PRP) or stem cells. None of these recent “novel” tendinopathy treatments have provided mechanistic insight; thus, their whole-hearted adoption in the clinical community is not yet apparent. Following PRP in the horse, there is experimental evidence of improved histology,<sup>35</sup> increased neovascularization,<sup>36</sup> and ultrasound appearance<sup>37</sup> of treated tendons, but clinical evidence has failed to show a treatment effect,<sup>38</sup> similar to the experience in human tendon disease.<sup>39</sup>

Following stem cells in the horse, there is experimental evidence of improved histology<sup>40,41</sup> and clinical evidence for safety,<sup>42</sup> improved cellularity,<sup>43</sup> and a reduced re-injury rate compared to historical controls.<sup>44</sup> The initial enthusiasm for stem cells in regenerative medicine was one of tissue-specific differentiation, in that stem cells implanted to a tendon lesion, for example, would engraft, become tenocytes, and produce tendon matrix. As both basic science and clinical data accumulate, it appears that stem cell therapy with the mesenchymal stem cell is due to local production of bioactive molecules and immune modulation rather than tissue-specific differentiation and long-term engraftment.<sup>45</sup> Herein, we show that local delivery of miR29a is capable of producing comparable and, in some cases, superior results to PRP or stem cell treatment (similar experimental trials), with regard to lesion size and histological improvement.<sup>46,47</sup> Our study appears to mirror the concept of earlier lesion resolution and lack of lesion progression at early time points. This, in conjunction with a concurrent tissue molecular phenotype of reduced collagen 3 confirmed macroscopically on T2 mapping, provides convincing evidence that a miR manipulation can target both inflammatory/matrix crosstalk in tendon disease, with subsequent lesion resolution. microRNAs have several important advantages in that they are bio-developable and comprise known sequences

and control arms of the study. The reduced expression of miR29a immediately after tendon injury up until 16 weeks post injury induction and concomitant increase in collagen 3:collagen 1 ratio in control animals that we report herein further demonstrates the model molecularly reflects disease in humans and in rodent models of tendinopathy.<sup>25</sup> The regulation of collagens and other extracellular matrices by the miR29 family has been highlighted in several prior studies.<sup>17,25,30</sup> Our results now show that miR29a acts as an important repressor to regulate collagen expression in equine tendon healing. The molecular understanding of increased collagen 3 deposition resulting in biomechanical inferiority and degeneration has been largely underinvestigated in equine tendon disease. Although it is likely that miR29a targets other important genes<sup>31,32</sup> in the multifaceted tendon injury milieu, our data suggest that miR29a is a critical driver of collagen post transcriptional regulation, resulting in a key collagen switch that remains a major pathological feature of equine tendinopathy. Novel quantitative biochemical MRI techniques, such as T2 mapping, have been increasingly evaluated for their demonstrated sensitivity in the detection of earlier biochemical changes (i.e., collagen bril structure, orientation, and water content) in various tissues.<sup>33,34</sup> Thus, the variability in T2 mapping of placebo-treated tendons as compared to miR-29a-treated tendons suggests improved

**Table 1. Subjective Ultrasound Scoring for Subcutaneous Thickening and Abnormal Tendon Shape**

Weeks	SC Thickening		Abnormal Shape	
	29a (%)	Control (%)	29a (%)	Control (%)
0	4/9 (44)	4/8 (50)	7/9 (78)	7/8 (88)
2	4/9 (44)	4/8 (50)	8/9 (89)	7/8 (88)
4	3/7 (43)	3/6 (50)	2/7 (29)	5/6 (83)
6	3/4 (75)	4/4 (100)	2/4 (50)	4/4 (100)
8	3/4 (75)	4/4 (100)	2/4 (50)	4/4 (100)
12	1/4 (25)	3/4 (75)	2/4 (50)	4/4 (100)
16	1/4 (25)	4/4 (100)	1/4 (25)	4/4 (100)

Each ultrasound image was scored by a blinded assessor (D.S.) for subcutaneous thickening (yes/no) or abnormal tendon shape (yes/no) at the site of induced injury.

that are often highly conserved among species, both attractive features from a drug development standpoint.

There are limitations inherent in our study. The equine model has the inability to test therapies in a large number of animals, resulting in a study that may be underpowered. This is due to the significant cost of housing, buying, and caring for these animals and the strong emotional and ethical considerations in their use and sacrifice.<sup>48</sup> We additionally note that due to logistical and ethical considerations, we were unable to completely age and sex match each animal within the treatment and placebo group. As mentioned, the collagenase model of tendon injury does not totally mimic the naturally occurring lesion in man. However, the collagenase model allows the generation of a homogeneous tendon lesion in a controlled group of animals and, therefore, improved ability to detect differences between the treated and control arms of the study. The equine mid-metacarpal SDFT is a large, weight-bearing tendon that is easily accessible, is not confined to a synovial sheath, and, in the equine athlete, is commonly affected by a naturally occurring over-stretch tendon injury compounded on previous microfiber disruption, similar to tendinopathies of the human Achilles tendon.<sup>49,50</sup> Finally, we appreciate that future studies should be conducted to further elucidate the ideal time of administration of any equine tendinopathy therapy. These studies would contribute to the understanding of when the best therapeutic results are obtained and whether it is feasible to prevent further injury when the therapy is administered to a still-developing injury.

## Conclusions

The present study demonstrated that a microRNA therapy had a favorable action in the treatment of tendinopathy by the prevention of lesion progression, improved tendon tissue quality, and histopathology comparable to current regenerative therapies. These data support the mechanism of microRNA-mediated modulation of early pathophysiologic events that facilitate tissue remodeling in the tendon after injury and provides a proof of principle that a locally delivered miR29a therapy can improve early tendon healing.

## MATERIALS AND METHODS

### Equine Model of Tendinopathy

#### Animals

The data generated in Figures 1 and 2 represent historical RNA tissue samples from a previously published model<sup>41</sup> and were utilized in the pursuit of RRR. Eight adult female Thoroughbred (n = 7) or Thoroughbred cross (n = 1) horses, ranging in age from 3 to 7 years, without clinical or ultrasonographic evidence of tendon injury, were used. All horses had undergone rigorous athletic training prior to inclusion in the study. Horses were housed separately, in box stalls, and allowed to acclimate to the environment for  $\geq 2$  weeks prior to study initiation. These animals then underwent the tendon injury model as described below.

For the randomized section of the trial, 17 adult Quarter-Horse-type horses, ranging in age from 2 to 7 years, without clinical or ultrasonographic evidence of tendon injury, were used. The sample size was based on the first authors previously published studies utilizing the collagenase model,<sup>41,51</sup> which showed the largest group should have eight horses to show statistical differences regarding tissue architecture, tendon size, tendon lesion size, and tendon linear fiber pattern. Horses were housed separately, in box stalls, and allowed to acclimate to the environment for  $\geq 2$  weeks prior to study initiation. All invasive procedures were performed by an experienced board-certified veterinary surgeon (A.E.W). This study was approved by and performed according to guidelines of the University's Institutional Animal Care and Use Committee, protocol number 2013-0019, and all experiments were performed in accordance with relevant guidelines and regulations.

#### Tendon Injury Induction and Therapy Administration

Collagenase-induced lesions were created in the tensile region of the SDFT of one randomly selected forelimb using filter sterilized bacterial collagenase type I (Sigma), as previously described.<sup>51</sup> Forelimb selection (left or right) was made by a coin toss for each horse. 1,000 U of collagenase was delivered to a columnar physical defect centered within the tensile region of the SDFT tendon (16–18 cm DACB) using a 16-gauge 8.89-cm Weiss Epidural needle with a Tuohy tip (BD) inserted under ultrasonographic guidance, as previously described. The study forelimb was bandaged. 1 week post tendon injury induction (0 weeks), tendons were injected with 1.5 mL of 100 nM miR29a (based on preliminary rodent in vivo studies) in PBS (modified to include 2'Fluoro and 2'O-Me nucleotides to increase half-life in serum) or placebo (PBS) via ultrasonographically guided intra-lesional injection in the mid-metacarpal lesion with 25-gauge needle entry at 17 cm DACB in the center of the lesion. The needle was directed from palmarolateral to dorsomedial.

#### Study Design

The study consisted of two randomly assigned groups: group A (miR29a mimic; n = 9; five males, four females; miR29a) and group B (placebo-treated tendons; n = 8; four males, four females; CONT). 1 week after tendon injury by collagenase injection, treatment injections were performed. A subset of animals was euthanized, and tissues were collected at 2, 4, and 16 weeks. Other than an on-site control officer, all investigators were blinded to treatment group

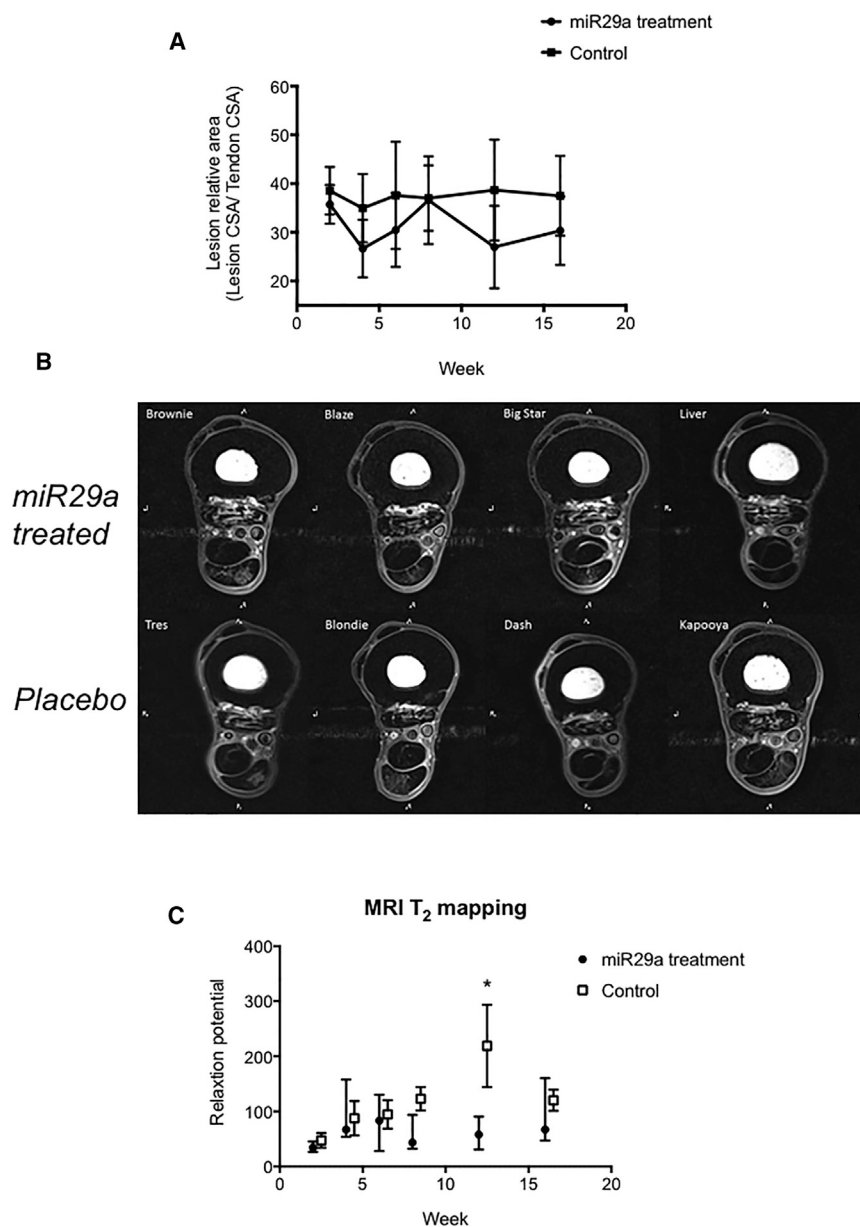


**Figure 5. MRI Tendon Healing Post miR29a Treatment**

(A) Normalized lesion to tendon CSA for miR29a- and placebo-treated tendons (control) at time points post treatment injection in weeks. (B) Transverse T<sub>1</sub> magnetic resonance images at 17 cm distal to the accessory carpal bone 16 weeks after treatment injection with miR29a- or placebo-treated tendons. (C) MRI T<sub>2</sub> r mapping relaxation times for miR29a- and placebo-treated tendons (control) at time points post treatment injection in weeks. \* $p < 0.05$  versus control (one-tailed Student's *t* test).

group, 16-week horse) had a mild flexural limb deformity (club foot) and one horse had delayed release of the patella (control group, 16-week horse). One horse (miR29a group, 16-week horse) got loose from her handler during the eighth week post-treatment injection and galloped free for 3 min. Other than one horse that was treated for colic prior to study initiation (miR29a group, week 4), none of the horses had a history of prior diseases or treatments other than castration, none required treatment for other diseases or injuries during the study, and there was no evidence of prior or concomitant diseases during post mortem examination in any of the horses. The age, sex, and weight of each animal are given in Table 2.

#### Ultrasound

Ultrasound examinations were performed prior to admission to the study (baseline) and at  $t = 0, 2, 4, 6, 8, 12,$  and 16 weeks after treatment injection. Ultrasound imaging was performed by a board-certified internal medicine specialist (D.S.) using a hospital-based non-portable ultrasound machine (MyLab 70, Esaote) equipped with a high frequency (4–13 MHz) linear array probe for equine tendon (LA523 Vet, Esaote). A template was used to ensure accurate repetition of tissue gain settings, focus,

and depth of tissue penetration. Longitudinal and transverse ultrasound images were acquired, and tendon cross-sectional area (TCSA), lesion cross-sectional area (LCSA), and a longitudinal linear fiber pattern score were measured by the same ultrasonographer at 16 cm DACB. The LCSA as a percentage of TCSA was calculated for relative lesion cross-sectional area (RLCSA). Tendons were also scored as having a normal shape (yes/no) and overlying subcutaneous thickening (yes/no).

#### MRI

MRI was performed at 2, 4, 6, 8, 12, and 16 weeks after treatment injection using a 3.0 Tesla MRI system (Siemens Magnetom Verio)

identification until the study was completed and all assays were performed. Treatment group (A or B) was revealed for statistical analysis. Once all analyses were completed, treatment group identification (miR29a or CONT) was disclosed.

None of the horses had been previously athletically trained. All horses had been housed at pasture in a group setting until 2 weeks prior to the start of the study, at which point they were housed individually in box stalls until study termination. 8 weeks post treatment injection, horses began daily in-hand walking exercise for 5 min, which was increased to 10 min a day for weeks 12–16. There were pre-existing musculoskeletal abnormalities in two horses: one horse (miR29a



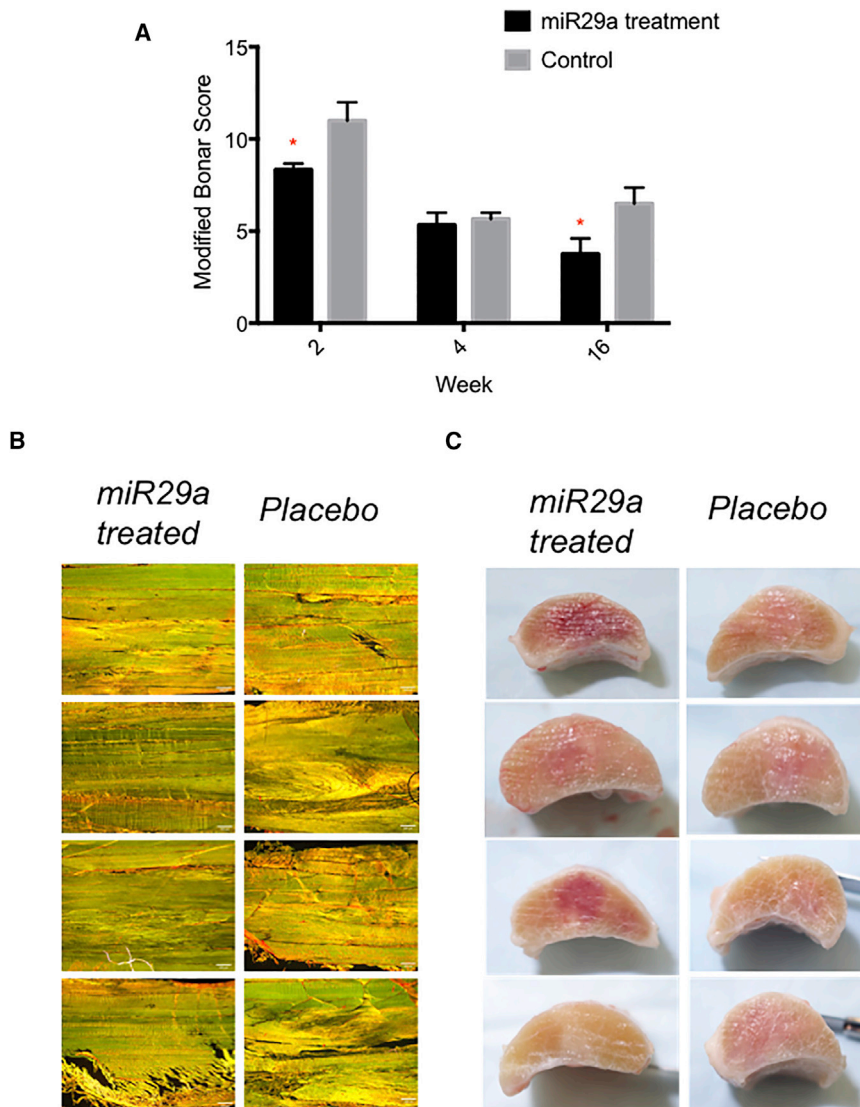


**Figure 6. Histology and Tissue Architecture Post miR29a Treatment**

(A) Histological scoring utilizing the modified Bonar score (cell density, vascularity, linear fiber, and polarized collagen) at 2, 4, and 16 weeks. \* $p < 0.05$  miR29a versus controls (Mann-Whitney U test). (B) 200 × magnification of longitudinal sections of superficial digital flexor tendon stained Picrosirius Red 16 weeks after treatment injection with miR29a- or placebo-treated tendons. Scale bar, 200 μm. (C) Cross sectional gross pathology images from miR29a-treated tendon versus control tendon at 16 weeks post treatment.

**Equine Tendon Explants**

To establish tendon explant cultures, the superficial digital flexor tendon was aseptically excised from the midmetacarpal region of both forelimbs of three horses (aged 2–5 years) without evidence or history of tendon injury; the horses were euthanized for reasons unrelated to the study. Tendons were determined to be normal on the basis of findings via palpation, gross examination, and later dissection for explant culture. Following collection, the tendon segments were maintained in culture medium during the removal of the paratenon. The tendon segments were then sectioned into 5- × 5- × 4-mm blocks and evenly distributed in 12-well plates for explant culture of tenocytes. Segments were maintained for 6 days at 37°C, 5% CO<sub>2</sub>, and 70% humidity in complete medium (penicillin [50 U/mL]; streptomycin [50 μg/mL]; ascorbic acid [100 μg/mL]; and 2% fetal bovine serum) to allow explant culture of tenocytes. After 6 days, each explant was divided, and a portion was snap frozen in liquid nitrogen

using a 15-channel knee coil (Quality Electrodynamics) and positioned in left lateral recumbency with a marker placed at 17 cm DACB. Sagittal and transverse plane T2 maps (i.e., turbo spin echo sequence with multiple echo times of 15.2, 30.4, 45.6, 60.8, 76, and 91.2 ms) and transverse plane STIR (short tau inversion recovery) images were acquired.

**Tissue Harvest**

Horses were euthanized by pentobarbital overdose at 2, 4, and 16 weeks post treatment injection. Limbs were dissected under RNase-free conditions, and samples were collected from the center of the tendon lesion at 16 cm DACB, extending into the surrounding normal tendon. Samples were snap frozen in liquid nitrogen, pulverized in a freezer mill, and stored at -80°C until use or fixed in 4% paraformaldehyde at 4°C for 72 hr.

and pulverized for RNA isolation with a phenol-guanidine isothiocyanate reagent. A cross-sectional edge was fixed in 4% paraformaldehyde, embedded in paraffin, and sectioned for H&E staining.

Equine tenocytes were transfected with Hsa-miR-29a-3p and miRIDIAN microRNA Negative Control #1 microRNA mimics using Dharmafect 3 (Dharmacon). Transfection efficiency was assessed using miRIDIANmimic Transfection control Dy-547 (Dharmacon). We determined the transfection efficiency using a fluorescently labeled miR29a mimic. This was performed initially in cultured human tenocytes, in which the uptake of labeled miR29a was monitored by fluorescent microscopy. Additionally, we assessed uptake of fluorescent miR29a when injected directly into the murine patellar tendon. In both cases, miR29a was readily taken up by tenocytes, with a transfection efficiency >85%.

**Table 2. Demographics of Horses Utilized in the Study**

Week	Group	Age	Sex	Weight (kg)	Height (cm)
2	A	4	M	413	142
2	A	3	M	394	147
2	A	3	F	412	147
2	B	4	M	468	147
2	B	6	F	558	160
4	A	6	F	404	142
4	A	6	F	432	147
4	B	2	M	492	157
4	B	2	M	484	155
16	A	3	M	408	147
16	A	2	F	424	147
16	A	2	M	436	147
16	A	4	F	466	152
16	B	4	M	452	150
16	B	3	M	402	147
16	B	6	F	420	147
16	B	2	M	443	145

Group A, miR29a treated; Group B, control, PBS. M, male; F, female.

### RNA and DNA Isolation and qPCR

The cells isolated from experiments and freezer mill pulverized tendon samples from the in vivo trial were placed in Trizol before mRNA extraction. QIAGEN mini columns (QIAGEN) were used for the RNA clean-up, with an incorporated on column DNase step as per the manufacturer's instructions. cDNA was prepared from RNA samples according to AffinityScript (Agilent Technologies) multiple temperature cDNA synthesis kit as per the manufacturer's instructions. Real-time PCR was performed using SYBR green or Taqman FastMix (Applied Biosystems) according to whether a probe was used with the primers. The cDNA was diluted 1 in 5 using RNase-free water. Each sample was analyzed in triplicate. Primers (Integrated DNA Technologies) were as follows:

GAPDH Forward 5'-AGAAGGAGAAAGGCCCTCAG-3' and Reverse 5'-GGAAACTGTGGAGGTCAGGA-3', Beta Actin Forward 5'-AAGGGACTTCCTGTAACAATGCA-3' and Reverse 5'-CTGGAACGGTGAAGGTGACA-3', Col1a1 Forward 5'-CAGACTGGCAACCTCAA GAA-3' and Reverse 5'-CAGACTGGCAACCTCAAGAA-3', Col3a1 Forward 5'-CTGGAGGATGGTTGCACTAAA-3' and Reverse 5'-CA CCAACATCATAGGGAGCAATA-3'

All mRNA and microRNA datasets represent fold change in gene expression compared with designated control utilizing housekeeping genes GAPDH, 18S, or U6, as detailed in the figure legend.

### RNA Isolation and qPCR of microRNA

Total RNA was isolated by miRNeasy kit (QIAGEN). miScript Reverse Transcription Kit (QIAGEN) was used for cDNA prepara-

tion. TaqMan mRNA assays (Applied Biosystems) or the miScript primer assay (QIAGEN) was used for quantitative determination of the expression of miR29a (MS00001701). Expressions of U6B small nuclear RNA or  $\beta$ -actin were used as endogenous controls.

### Luciferase Assay

Conserved miR29a-binding sites in the 3' UTRs of equine col1a1 and col3a1 were identified using TargetScan. The regions corresponding to these sites were synthesized as G-blocks (Integrated DNA Technologies) and inserted downstream of the luciferase ORF in pmirGLO (Promega) using Gibson Assembly (New England Biolabs). The equivalent regions, in which the seed regions of predicted miR29a-binding sites were deleted, were created in parallel. Plasmids were transfected into HEK293 cells, along with miR29a or scrambled control mimics (Thermo Fisher Scientific), using Attractene (QIAGEN). Luciferase activities were measured using Dual-Glo luciferase assay (Promega).

### 3' RACE

3' UTR sequences of col1a1 and col3a1 transcripts were generated by 3' RACE by using RNA prepared from equine tenocytes. The primers used were as follows: col1a1 GSP1 5'-CCCTGGAAACAGACAAA CAAC-3', col1a1 GSP2 5'-CAGACAAAACAACCCAAACTGAA-3', col3a1 GSP1 5'-AGGCCGTGAGACTACCTATT-3' and col3a1 GSP2 5'-CTATGATGTTGGTGGTCTGAT-3'. The resulting PCR products were cloned into pCR2.1 TOPO (Invitrogen) for sequencing.

### Histology

Fixed longitudinal tissue sections were embedded in paraffin, sectioned, and stained with H&E or Picrosirius Red and examined under white light and polarized light microscopy. All slides were examined by a board-certified veterinary pathologist who specialized in musculoskeletal pathology (R.P.). Sections were sequentially examined across and down the entire tendon section under low power and high power (ten fields), where appropriate, for cell detail to derive a complete histologic impression. All tendon parameters were scored from 1 (normal) to 4 (severe changes) for tenocyte shape, tenocyte density, free hemorrhage, neovascularization, perivascular cuffing, collagen fiber linearity, collagen fiber uniformity, and polarized light crimping, as previously described.<sup>51</sup>

### Statistical Analyses

All results are shown as mean  $\pm$  SEM, and all statistical analysis was performed using Student's t test, ANOVA, or Mann-Whitney U test, as indicated in the figure legends, using the GraphPad Prism 5 software. A p value of < 0.05 was considered statistically significant.

### AUTHOR CONTRIBUTIONS

N.L.M., A.E.W., D.S.G., and T.H. conceived and designed the experiments. N.L.M., D.S.G., S.M.K. M.A., R.R., J.G., and R.P., performed the experiments. T.H. and I.B.M. provided expert advice. All authors analyzed the data. N.L.M., A.E.W., and D.S.G. wrote the paper.

## CONFLICTS OF INTEREST

The authors declare no competing financial interests. The University of Glasgow has applied for a patent to cover the use of microRNA29 in tendon injury.

## ACKNOWLEDGMENTS

All procedures and protocols were approved by the Institutional Animal Care and Use Committee, protocol number 2013-0019. N.L.M., A.E.W., and D.S.G. have access to all the data, and data are available upon request.

## REFERENCES

- Battery, L., and Maffulli, N. (2011). Inflammation in overuse tendon injuries. *Sports Med. Arthrosc. Rev.* 19, 213–217.
- Birch, H.L. (2007). Tendon matrix composition and turnover in relation to functional requirements. *Int. J. Exp. Pathol.* 88, 241–248.
- Dakin, S.G., Werling, D., Hibbert, A., Abayasekara, D.R., Young, N.J., Smith, R.K., and Dudhia, J. (2012). Macrophage sub-populations and the lipoxin A4 receptor implicate active inflammation during equine tendon repair. *PLoS ONE* 7, e32333.
- Hyman, J., and Rodeo, S.A. (2000). Injury and repair of tendons and ligaments. *Phys. Med. Rehabil. Clin. N. Am.* 11, 267–288, v.
- Goodship, A.E. (1993). The pathophysiology of flexor tendon injury in the horse. *Equine Vet. Educ.* 5, 23–29.
- Kasashima, Y., Takahashi, T., Smith, R.K., Goodship, A.E., Kuwano, A., Ueno, T., and Hirano, S. (2004). Prevalence of superficial digital flexor tendonitis and suspensory desmitis in Japanese Thoroughbred flat racehorses in 1999. *Equine Vet. J.* 36, 346–350.
- Millar, N.L., Hueber, A.J., Reilly, J.H., Xu, Y., Fazzi, U.G., Murrell, G.A., and McInnes, I.B. (2010). Inflammation is present in early human tendinopathy. *Am. J. Sports Med.* 38, 2085–2091.
- Millar, N.L., Dean, B.J., and Dakin, S.G. (2016). Inflammation and the continuum model: time to acknowledge the molecular era of tendinopathy. *Br. J. Sports Med.*, Published online June 3, 2016. <http://dx.doi.org/10.1136/bjsports-2016-096419>.
- Millar, N.L., Murrell, G.A.C., and McInnes, I.B. (2017). Inflammatory mechanisms in tendinopathy - towards translation. *Nat. Rev. Rheumatol.* 13, 110–122.
- Dakin, S.G., Martinez, F.O., Yapp, C., Wells, G., Oppermann, U., Dean, B.J., Smith, R.D., Whewy, K., Watkins, B., Roche, L., et al. (2015). Inflammation activation and resolution in human tendon disease. *Sci. Transl. Med.* 7, 311ra173.
- Behzad, H., Sharma, A., Mousavizadeh, R., Lu, A., and Scott, A. (2013). Mast cells exert pro-inflammatory effects of relevance to the pathophysiology of tendinopathy. *Arthritis Res. Ther.* 15, R184.
- John, T., Lodka, D., Kohl, B., Ertel, W., Jammrath, J., Conrad, C., Stoll, C., Busch, C., and Schulze-Tanzil, G. (2010). Effect of pro-inflammatory and immunoregulatory cytokines on human tenocytes. *J. Orthop. Res.* 28, 1071–1077.
- Dakin, S.G., Dudhia, J., and Smith, R.K. (2013). Science in brief: resolving tendon inflammation. A new perspective. *Equine Vet. J.* 45, 398–400.
- Dakin, S.G., Dudhia, J., Werling, N.J., Werling, D., Abayasekara, D.R., and Smith, R.K. (2012). Inflammation-aging and arachadonic acid metabolite differences with stage of tendon disease. *PLoS ONE* 7, e48978.
- Millar, N.L., Akbar, M., Campbell, A.L., Reilly, J.H., Kerr, S.C., McLean, M., Frleta-Gilchrist, M., Fazzi, U.G., Leach, W.J., Rooney, B.P., et al. (2016). IL-17A mediates inflammatory and tissue remodelling events in early human tendinopathy. *Sci. Rep.* 6, 27149.
- He, L., and Hannon, G.J. (2004). MicroRNAs: small RNAs with a big role in gene regulation. *Nat. Rev. Genet.* 5, 522–531.
- Maurer, B., Stanczyk, J., Jünger, A., Akhmetshina, A., Trenkmann, M., Brock, M., Kowal-Bielecka, O., Gay, R.E., Michel, B.A., Distler, J.H., et al. (2010). MicroRNA-29, a key regulator of collagen expression in systemic sclerosis. *Arthritis Rheum.* 62, 1733–1743.
- Kurowska-Stolarska, M., Alivernini, S., Ballantine, L.E., Asquith, D.L., Millar, N.L., Gilchrist, D.S., Reilly, J., Ierna, M., Fraser, A.R., Stolarski, B., et al. (2011). MicroRNA-155 as a proinflammatory regulator in clinical and experimental arthritis. *Proc. Natl. Acad. Sci. USA* 108, 11193–11198.
- Bushati, N., and Cohen, S.M. (2007). microRNA functions. *Annu. Rev. Cell Dev. Biol.* 23, 175–205.
- Bartel, D.P. (2009). MicroRNAs: target recognition and regulatory functions. *Cell* 136, 215–233.
- Zeng, L., He, X., Wang, Y., Tang, Y., Zheng, C., Cai, H., Liu, J., Wang, Y., Fu, Y., and Yang, G.Y. (2014). MicroRNA-210 overexpression induces angiogenesis and neurogenesis in the normal adult mouse brain. *Gene Ther.* 21, 37–43.
- Usman, M.A., Nakasa, T., Shoji, T., Kato, T., Kawanishi, Y., Hamanishi, M., Kamei, N., and Ochi, M. (2015). The effect of administration of double stranded MicroRNA-210 on acceleration of Achilles tendon healing in a rat model. *J. Orthop. Sci.* 20, 538–546.
- Chen, C.H., Zhou, Y.L., Wu, Y.F., Cao, Y., Gao, J.S., and Tang, J.B. (2009). Effectiveness of microRNA in down-regulation of TGF-beta gene expression in digital flexor tendons of chickens: in vitro and in vivo study. *J. Hand Surg. Am.* 34, 1777–1784.e1.
- Chen, Q., Lu, H., and Yang, H. (2014). Chitosan inhibits fibroblasts growth in Achilles tendon via TGF-β1/Smad3 pathway by miR-29b. *Int. J. Clin. Exp. Pathol.* 7, 8462–8470.
- Millar, N.L., Gilchrist, D.S., Akbar, M., Reilly, J.H., Kerr, S.C., Campbell, A.L., Murrell, G.A., Liew, F.Y., Kurowska-Stolarska, M., and McInnes, I.B. (2015). MicroRNA29a regulates IL-33-mediated tissue remodelling in tendon disease. *Nat. Commun.* 6, 6774.
- Brown, B.D., and Naldini, L. (2009). Exploiting and antagonizing microRNA regulation for therapeutic and experimental applications. *Nat. Rev. Genet.* 10, 578–585.
- Abonnenc, M., Nabeebaccus, A.A., Mayr, U., Barallobre-Barreiro, J., Dong, X., Cuellar, F., Sur, S., Drozdov, I., Langley, S.R., Lu, R., et al. (2013). Extracellular matrix secretion by cardiac fibroblasts: role of microRNA-29b and microRNA-30c. *Circ. Res.* 113, 1138–1147.
- Williams, I.F., McCullagh, K.G., Goodship, A.E., and Silver, I.A. (1984). Studies on the pathogenesis of equine tendonitis following collagenase injury. *Res. Vet. Sci.* 36, 326–338.
- Lake, S.P., Anson, H.L., and Soslowsky, L.J. (2008). Animal models of tendinopathy. *Disabil. Rehabil.* 30, 1530–1541.
- Sengupta, S., den Boon, J.A., Chen, I.H., Newton, M.A., Stanhope, S.A., Cheng, Y.J., Chen, C.J., Hildesheim, A., Sugden, B., and Ahlquist, P. (2008). MicroRNA 29c is down-regulated in nasopharyngeal carcinomas, up-regulating mRNAs encoding extracellular matrix proteins. *Proc. Natl. Acad. Sci. USA* 105, 5874–5878.
- Qin, W., Chung, A.C., Huang, X.R., Meng, X.M., Hui, D.S., Yu, C.M., Sung, J.J., and Lan, H.Y. (2011). TGF-β/Smad3 signaling promotes renal fibrosis by inhibiting miR-29. *J. Am. Soc. Nephrol.* 22, 1462–1474.
- Ciechomska, M., O'Reilly, S., Suwara, M., Bogunia-Kubik, K., and van Laar, J.M. (2014). MiR-29a reduces TIMP-1 production by dermal fibroblasts via targeting TGF-β activated kinase 1 binding protein 1, implications for systemic sclerosis. *PLoS ONE* 9, e115596.
- Ganal, E., Ho, C.P., Wilson, K.J., Surowiec, R.K., Smith, W.S., Dornan, G.J., and Millett, P.J. (2016). Quantitative MRI characterization of arthroscopically verified supraspinatus pathology: comparison of tendon tears, tendinosis and asymptomatic supraspinatus tendons with T2 mapping. *Knee Surg. Sports Traumatol. Arthrosc.* 24, 2216–2224.
- Bangerter, N.K., Taylor, M.D., Tarbox, G.J., Palmer, A.J., and Park, D.J. (2016). Quantitative techniques for musculoskeletal MRI at 7 Tesla. *Quant. Imaging Med. Surg.* 6, 715–730.
- van Schie, H.T., Bakker, E.M., Cherdchutham, W., Jonker, A.M., van de Lest, C.H., and van Weeren, P.R. (2009). Monitoring of the repair process of surgically created lesions in equine superficial digital flexor tendons by use of computerized ultrasonography. *Am. J. Vet. Res.* 70, 37–48.
- Bosch, G., Moleman, M., Barneveld, A., van Weeren, P.R., and van Schie, H.T. (2010). The effect of platelet-rich plasma on the neovascularization of surgically created equine superficial digital flexor tendon lesions. *Scand. J. Med. Sci. Sports* 21, 554–561.

37. Bosch, G., René van Weeren, P., Barneveld, A., and van Schie, H.T. (2011). Computerised analysis of standardised ultrasonographic images to monitor the repair of surgically created core lesions in equine superficial digital flexor tendons following treatment with intratendinous platelet rich plasma or placebo. *Vet. J.* 187, 92–98.
38. Garrett, K.S., Bramlage, L.R., Spike-Pierce, D.L., and Cohen, N.D. (2013). Injection of platelet- and leukocyte-rich plasma at the junction of the proximal sesamoid bone and the suspensory ligament branch for treatment of yearling Thoroughbreds with proximal sesamoid bone inflammation and associated suspensory ligament branch desmitis. *J. Am. Vet. Med. Assoc.* 243, 120–125.
39. de Vos, R.J., Weir, A., van Schie, H.T., Bierma-Zeinstra, S.M., Verhaar, J.A., Weinans, H., and Tol, J.L. (2010). Platelet-rich plasma injection for chronic Achilles tendinopathy: a randomized controlled trial. *JAMA* 303, 144–149.
40. Nixon, A.J., Dahlgren, L.A., Haupt, J.L., Yeager, A.E., and Ward, D.L. (2008). Effect of adipose-derived nucleated cell fractions on tendon repair in horses with collagenase-induced tendinitis. *Am. J. Vet. Res.* 69, 928–937.
41. Watts, A.E., Yeager, A.E., Kopyov, O.V., and Nixon, A.J. (2011). Fetal derived embryonic-like stem cells improve healing in a large animal flexor tendonitis model. *Stem Cell Res. Ther.* 2, 4.
42. Pacini, S., Spinabella, S., Trombi, L., Fazzi, R., Galimberti, S., Dini, F., Carlucci, F., and Petrini, M. (2007). Suspension of bone marrow-derived undifferentiated mesenchymal stromal cells for repair of superficial digital flexor tendon in race horses. *Tissue Eng.* 13, 2949–2955.
43. Smith, R.K., Werling, N.J., Dakin, S.G., Alam, R., Goodship, A.E., and Dudhia, J. (2013). Beneficial effects of autologous bone marrow-derived mesenchymal stem cells in naturally occurring tendinopathy. *PLoS ONE* 8, e75697.
44. Godwin, E.E., Young, N.J., Dudhia, J., Beamish, I.C., and Smith, R.K. (2012). Implantation of bone marrow-derived mesenchymal stem cells demonstrates improved outcome in horses with overstrain injury of the superficial digital flexor tendon. *Equine Vet. J.* 44, 25–32.
45. Caplan, A.I., and Correa, D. (2011). The MSC: an injury drugstore. *Cell Stem Cell* 9, 11–15.
46. Carvalho Ade, M., Badial, P.R., Álvarez, L.E., Yamada, A.L., Borges, A.S., Deffune, E., Hussni, C.A., and Garcia Alves, A.L. (2013). Equine tendonitis therapy using mesenchymal stem cells and platelet concentrates: a randomized controlled trial. *Stem Cell Res. Ther.* 4, 85.
47. de Mattos Carvalho, A., Garcia Alves, A.L., Galvão Gomes de Oliveira, P., Cisneros Álvarez, L.E., Amorim, R.L., Hussni, C.A., and Deffune, E. (2011). Use of adipose tissue-derived mesenchymal stem cells for experimental tendinitis therapy in equines. *J. Equine Vet. Sci.* 31, 26–34.
48. Koch, T.G., and Betts, D.H. (2007). Stem cell therapy for joint problems using the horse as a clinically relevant animal model. *Expert Opin. Biol. Ther.* 7, 1621–1626.
49. Abate, M., Silbernagel, K.G., Siljeholm, C., Di Iorio, A., De Amicis, D., Salini, V., Werner, S., and Paganelli, R. (2009). Pathogenesis of tendinopathies: inflammation or degeneration? *Arthritis Res. Ther.* 11, 235.
50. Dowling, B.A., Dart, A.J., Hodgson, D.R., and Smith, R.K.W. (2000). Superficial digital flexor tendonitis in the horse. *Equine Vet. J.* 32, 369–378.
51. Watts, A.E., Nixon, A.J., Yeager, A.E., and Mohammed, H.O. (2012). A collagenase gel/physical defect model for controlled induction of superficial digital flexor tendonitis. *Equine Vet. J.* 44, 576–586.